

LLDE: ENHANCING LOW-LIGHT IMAGES WITH DIFFUSION MODEL

Xin Peng Ooi and Chee Seng Chan*

CISiP, Faculty of Comp. Sci. and Info. Tech., Universiti Malaya, Kuala Lumpur, Malaysia

ABSTRACT

Limited generalization capability has been an unsolved issue in the domain of low-light image enhancement. Many models find enhancing out-of-distribution underexposed images challenging. In this work, we offer a fresh point of view on this issue. Our approach involves dividing the enhancement process into many small steps and performing them gradually. This method allows the model to acquire a more robust understanding of the data. To put this concept into practice, we proposed to adopt a diffusion model for low-light image enhancement, as its way of encoding the mapping between the source and target distributions fits our idea. Empirically, we show that our proposed model (LLDE) can outperform recent SOTAs quantitatively and visually. The code is publicly available at <https://github.com/OoiXinPeng/LLDE>.

Index Terms— low-light image enhancement, denoising diffusion models

1. INTRODUCTION

Images with inadequate illumination are often regarded as low-quality or degraded, and extracting desired information from such images is very challenging. However, such phenomena are unavoidable in real life, *e.g.* autonomous cars often need to capture and process road conditions at night or when surrounding lighting is poor.

In order to improve the quality of images taken in low-light conditions, much research has been investigated. Despite some impressive results, they tend to suffer from limited generalization capability [1]. One of the reasons for this is that the publicly available training datasets are small, causing the models to struggle with uncommon ill-illuminated situations that they were not trained on.

In this paper, we bring a new perspective to the field of low-light image enhancement. Intuitively, we believe that breaking down the enhancement process into small steps and gradually executing them will enable the model to learn a more robust representation of the data, ultimately improving the enhancement results of underexposed images that fall outside the training distribution. To align with this concept, we adopt a diffusion model [2, 3], as its approach of encoding a latent mapping between the source and target distributions

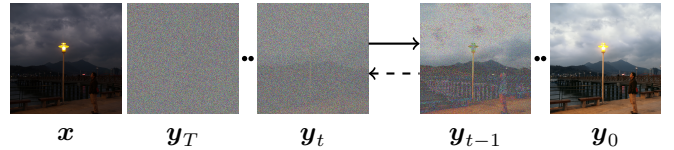


Fig. 1. Forward diffusion $q(\mathbf{y}_t \mid \mathbf{y}_{t-1})$ (dashed arrow) gradually corrupts the target normal-light image \mathbf{y}_0 . Guided by the learned latent space of normal-light image distribution, conditional reverse diffusion $p_\theta(\mathbf{y}_{t-1} \mid \mathbf{y}_t, \mathbf{x})$ (solid arrow) iteratively estimates the noise to neutralize the noise injected and enhance the input low-light image \mathbf{x} .

supports our idea, as illustrated in Fig. 1. Empirical results on two public datasets in four different quantitative metrics show the effectiveness of our proposed method.

2. RELATED WORK

2.1. Low-Light Image Enhancement

Low-light image enhancement has been a popular research area for many years. Traditional methods, such as Histogram Equalization (HE) [4] and Retinex-based algorithms [5] have limitations such as amplified noise in the enhanced images. To overcome these issues, researchers proposed deep learning-based enhancement methods, which can be classified into CNN-based and generative-based methods.

Many CNN-based methods are inspired by Retinex theory [5]. Their design involves estimating the illumination and reflectance of the input low-light images. For example, Zhang *et al.* proposed a multi-scale illumination attention module to reduce visual defects. Liu *et al.* [6] built an unrolling framework for both illumination estimation and noise removal. In addition, SCI [7] introduced a cascaded illumination learning process with weight sharing. Meanwhile, ZeroDCE++ [8] built quadratic curve estimation networks with specially designed unsupervised loss functions.

Meanwhile, generative-based methods aim to model the underlying mapping between low-light and normal-light distributions. Jiang *et al.* [9] proposed an unsupervised GAN-based method that uses unpaired low/normal-light images in training. On the other hand, Wang *et al.* [10] built a normalizing flow network to model the one-to-many relationship.

*Corresponding author / Email: cs.chan@um.edu.my

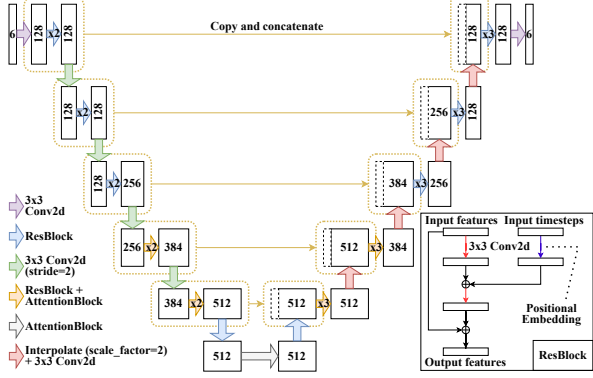


Fig. 2. Simplified illustration of our LLDE’s architecture. The number in the white box indicates the feature map’s channel dimension where six dimensional input is the concatenation of \mathbf{x} and \mathbf{y}_t , while 6 dimensional output is $\epsilon_\theta(\mathbf{y}_t, \mathbf{x}, t)$ and \mathbf{v} .

2.2. Diffusion Probabilistic Models

Recently, diffusion probabilistic models [2, 3] have received increasing attention from the academic community due to their excellent image generation capabilities, and many efforts [11, 12] have been studied to improve them. The basic idea is to gradually corrupt the input image using Gaussian noise, until it is in-distinguishable from Gaussian noise. Then, the model is trained to denoise the corrupted image gradually until the original image is recovered. By learning this reverse process, the diffusion model can sample new images from the desired distribution.

Furthermore, conditional diffusion models start to shine in various downstream computer vision tasks, including class-conditional image generation [13], super-resolution [14], weather conditions removal [15] and star field image enhancement [16]. These successful examples instill the belief that diffusion models will be effective in general low-light image enhancement.

3. METHODOLOGY

3.1. Denoising Diffusion Probabilistic Models

Denoising diffusion probabilistic models (DDPM) [3] define a forward diffusion process q that gradually injects Gaussian noise into images $\mathbf{y}_0 \sim q(\mathbf{y}_0)$ over T diffusion time steps in a Markovian manner. In our case, \mathbf{y}_0 are clean normal-light images as we want to learn their latent space. This noise injection follows a predefined linear variance schedule $\beta_1 < \dots < \beta_T$, where $\beta_t \in (0, 1)$:

$$q(\mathbf{y}_t | \mathbf{y}_{t-1}) = \mathcal{N}(\mathbf{y}_t; \sqrt{1 - \beta_t} \mathbf{y}_{t-1}, \beta_t \mathbf{I}) \quad (1)$$

$$q(\mathbf{y}_{1:T} | \mathbf{y}_0) = \prod_{t=1}^T q(\mathbf{y}_t | \mathbf{y}_{t-1}) \quad (2)$$

As mentioned in [3], we can directly sample any intermediate noisy normal-light images \mathbf{y}_t with $\alpha_t = 1 - \beta_t$ and $\bar{\alpha}_t = \prod_{i=1}^t \alpha_i$:

$$q(\mathbf{y}_t | \mathbf{y}_0) = \mathcal{N}(\mathbf{y}_t; \sqrt{\bar{\alpha}_t} \mathbf{y}_0, (1 - \bar{\alpha}_t) \mathbf{I}) \quad (3)$$

$$\mathbf{y}_t = \sqrt{\bar{\alpha}_t} \mathbf{y}_0 + \sqrt{1 - \bar{\alpha}_t} \boldsymbol{\epsilon}_t \quad (4)$$

where $\boldsymbol{\epsilon}_t \sim \mathcal{N}(\mathbf{0}, \mathbf{I})$. This enables the neural networks to be trained at arbitrary diffusion time steps.

To be tractable, we need to condition the posterior distribution $q(\mathbf{y}_{t-1} | \mathbf{y}_t)$ on \mathbf{y}_0 . It can be derived using the Bayes theorem and some algebraic manipulation as follows:

$$q(\mathbf{y}_{t-1} | \mathbf{y}_t, \mathbf{y}_0) = \mathcal{N}(\mathbf{y}_{t-1}; \tilde{\mu}_t(\mathbf{y}_t, t), \tilde{\beta}_t \mathbf{I}) \quad (5)$$

where the mean and variance are:

$$\tilde{\mu}_t(\mathbf{y}_t, t) = \frac{1}{\sqrt{\bar{\alpha}_t}} \left(\mathbf{y}_t - \frac{\beta_t}{\sqrt{1 - \bar{\alpha}_t}} \boldsymbol{\epsilon}_t \right), \quad \tilde{\beta}_t = \frac{1 - \bar{\alpha}_{t-1}}{1 - \bar{\alpha}_t} \beta_t \quad (6)$$

The reverse diffusion process p is a process of approximating the posterior distribution. In other words, it gradually recovers normal-lights image from noise. It starts from the prior $p(\mathbf{y}_T) = \mathcal{N}(\mathbf{y}_T; \mathbf{0}, \mathbf{I})$ using a neural network:

$$p_\theta(\mathbf{y}_{t-1} | \mathbf{y}_t) = \mathcal{N}(\mathbf{y}_{t-1}; \mu_\theta(\mathbf{y}_t, t), \Sigma_\theta(\mathbf{y}_t, t)) \quad (7)$$

$$p_\theta(\mathbf{y}_{0:T}) = p(\mathbf{y}_T) \prod_{t=1}^T p_\theta(\mathbf{y}_{t-1} | \mathbf{y}_t) \quad (8)$$

The combination of the conditioned posterior distribution and the reverse diffusion process can be viewed as a variational autoencoder [17]. As such, the model can be trained by optimizing the variational lower bound:

$$L_{\text{vlb}} = \mathbb{E}_q \underbrace{[D_{\text{KL}}(q(\mathbf{y}_T | \mathbf{y}_0) \| p(\mathbf{y}_T))]_{L_T}}_{L_0} - \log p_\theta(\mathbf{y}_0 | \mathbf{y}_1) + \sum_{t>1} \underbrace{D_{\text{KL}}(q(\mathbf{y}_{t-1} | \mathbf{y}_t, \mathbf{y}_0) \| p_\theta(\mathbf{y}_{t-1} | \mathbf{y}_t))}_{L_{t-1}} \quad (9)$$

In [3], $\Sigma_\theta(\mathbf{y}_t, t)$ in reverse diffusion process is not learned but fixed to $\sigma_t^2 \mathbf{I}$, where σ_t^2 can be β_t or $\tilde{\beta}_t$. Similarly to Equation 6, the mean is parameterized as:

$$\mu_\theta(\mathbf{y}_t, t) = \frac{1}{\sqrt{\bar{\alpha}_t}} \left(\mathbf{y}_t - \frac{\beta_t}{\sqrt{1 - \bar{\alpha}_t}} \boldsymbol{\epsilon}_\theta(\mathbf{y}_t, t) \right) \quad (10)$$

where the neural network is trained to predict the noise vector. With this parameterization, the training objective is reweighted and simplified to:

$$L_{\text{simple}} = \mathbb{E}_{t, \mathbf{y}_0, \boldsymbol{\epsilon}_t} [\|\boldsymbol{\epsilon}_t - \boldsymbol{\epsilon}_\theta(\mathbf{y}_t, t)\|^2] \quad (11)$$

To generate new normal-light images \mathbf{y}_0 , we use the trained neural network to sample $\mathbf{y}_{t-1} \sim p_\theta(\mathbf{y}_{t-1} | \mathbf{y}_t)$ iteratively, starting from $\mathbf{y}_T \sim \mathcal{N}(\mathbf{0}, \mathbf{I})$ as follows:

$$\mathbf{y}_{t-1} = \frac{1}{\sqrt{\bar{\alpha}_t}} \left(\mathbf{y}_t - \frac{\beta_t}{\sqrt{1 - \bar{\alpha}_t}} \boldsymbol{\epsilon}_\theta(\mathbf{y}_t, t) \right) + \sigma_t \mathbf{z} \quad (12)$$

where $\mathbf{z} \sim \mathcal{N}(\mathbf{0}, \mathbf{I})$.

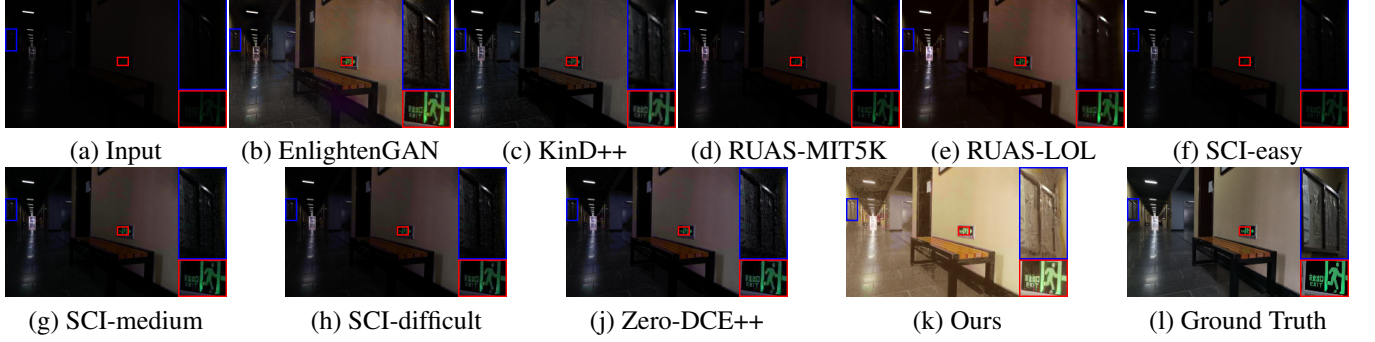


Fig. 3. Visual comparisons on a challenging low-light image selected from the LSRW dataset.

3.2. Conditional Diffusion Probabilistic Models

Similar to other generative models, diffusion probabilistic models can be used to model the underlying mapping between input low light images \mathbf{x} and their corresponding target normal-light images \mathbf{y} to perform an image translation task. This can be achieved by performing forward diffusion $q(\mathbf{y}_{1:T} \mid \mathbf{y}_0)$ to the target normal-light images like the original DDPM, and learning to sample from the posterior distribution while conditioned on the input low-light images (refer to Figure 1). *We argue that the enhancement is divided into many small steps in this process. The model learns to perform it gradually to the input low-light images, guided by the latent space of normal-light image distribution.* The conditional reverse diffusion process is defined as:

$$p_{\theta}(\mathbf{y}_{0:T} \mid \mathbf{x}) = p(\mathbf{y}_T) \prod_{t=1}^T p_{\theta}(\mathbf{y}_{t-1} \mid \mathbf{y}_t, \mathbf{x}) \quad (13)$$

$$p_{\theta}(\mathbf{y}_{t-1} \mid \mathbf{y}_t, \mathbf{x}) = \mathcal{N}(\mathbf{y}_{t-1}; \boldsymbol{\mu}_{\theta}(\mathbf{y}_t, \mathbf{x}, t), \boldsymbol{\Sigma}_{\theta}(\mathbf{y}_t, \mathbf{x}, t)) \quad (14)$$

Consequently, the noise $\epsilon_{\theta}(\mathbf{y}_t, t)$ in Equations 10, 11 and 12 is updated to $\epsilon_{\theta}(\mathbf{y}_t, \mathbf{x}, t)$.

3.3. LLDE: Low-Light Diffusive Enhancement

Like other image-to-image translation diffusion models [14–16], we choose to condition the input low-light image \mathbf{x} in the reverse diffusion process by concatenating it with noisy enhanced output \mathbf{y}_t . LLDE uses a UNet-like network [18] similar to [3] with some changes to the attention layers referred from [13]. The model architecture is illustrated in Figure 2.

Furthermore, in order to produce more visually appealing enhanced images, we have incorporated two techniques from [12] into LLDE. The first technique involves utilizing a cosine variance schedule instead of a linear schedule, thereby ensuring smoother forward and reverse diffusion processes. The second technique involves learning a vector \mathbf{v} to predict the variance in the reverse diffusion process as follows:

$$\Sigma_{\theta}(\mathbf{y}_t, \mathbf{x}, t) = \exp(\mathbf{v} \log \beta_t + (1 - \mathbf{v}) \log \tilde{\beta}_t) \quad (15)$$

As a result, the training objective is updated to:

$$\mathcal{L}_{\theta} = L_{\text{simple}} + \lambda L_{\text{vib}} \quad (16)$$

and σ_t in Equation 12 is updated to $\sigma_{\theta}(\mathbf{y}_t, \mathbf{x}, t)$.

4. EXPERIMENTS

4.1. Datasets

For training, we use all the 500 paired low/normal-light images from the LOL dataset [19]. For quantitative evaluation, we use 50 low-light test images from the LSRW dataset [20], and their corresponding normal-light images are the ground truth for the full reference metrics. In addition to the LSRW dataset, we also sample images from the NPE dataset [21] for visual comparisons.

4.2. Implementation details

All training images are resized, cropped to 128×128 and randomly flipped horizontally. The model is trained for 150k iterations using the Adam optimizer at a fixed learning rate of 10^{-4} without weight decay. An exponential moving average (EMA) is implemented over model parameters with a rate of 0.9999 for a more stable training. The dropout value is 0.3 for the ResNet blocks in the model. The number of diffusion steps T is 1000, similar to DDPM [3]. The training batch size is 32 and the entire training process is performed on a single NVIDIA Tesla V100s GPU.

For testing, in order to reduce the enhancement time, we adopt the sampling strategy proposed in [12]. We decrease the diffusion time steps T from 1000 to 25, and select a list of 25 evenly distributed time steps τ , ranging from 1 to 1000 with both endpoints included. The sampling variances for each new time step τ are as follows:

$$\beta_{\tau} = 1 - \frac{\bar{\alpha}_{\tau}}{\bar{\alpha}_{\tau-1}}, \quad \tilde{\beta}_{\tau} = \frac{1 - \bar{\alpha}_{\tau-1}}{1 - \bar{\alpha}_{\tau}} \beta_{\tau} \quad (17)$$

and Equation 14 is updated to:

$$p_{\theta}(\mathbf{y}_{\tau-1} \mid \mathbf{y}_{\tau}, \mathbf{x}) = \mathcal{N}(\mathbf{y}_{\tau-1}; \boldsymbol{\mu}_{\theta}(\mathbf{y}_{\tau}, \mathbf{x}, \tau), \boldsymbol{\Sigma}_{\theta}(\mathbf{y}_{\tau}, \mathbf{x}, \tau)) \quad (18)$$

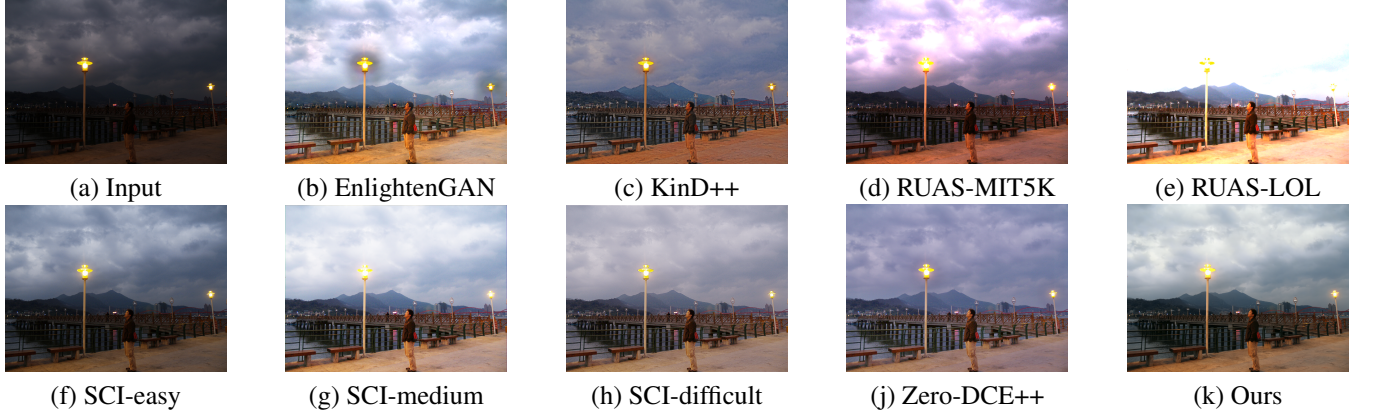


Fig. 4. Visual comparisons on an underexposed image sampled from the NPE dataset.

Table 1. Comparison results on LSRW dataset. For each metric, the **best** result is bold and the second best result is underlined.

Methods	PSNR↑	SSIM↑	LPIPS↓	NIQE↓
EnlightenGAN [9]	17.1039	0.5037	0.3270	3.4847
KinD++ [22]	16.1745	0.4422	0.3468	3.4126
RUAS-MIT5K [6]	13.0702	0.3791	0.3777	4.2689
RUAS-LOL [6]	14.2904	<u>0.5237</u>	0.4659	5.4262
SCI-easy [7]	11.8472	0.3313	0.3976	4.3690
SCI-medium [7]	15.2718	0.4484	0.3219	3.8473
SCI-difficult [7]	15.2093	0.4313	0.3254	3.9185
Zero-DCE++ [8]	16.2833	0.4844	<u>0.3175</u>	3.7678
Ours	16.7430	0.5301	0.3045	3.9306

4.3. Results and Comparison

In the LSRW dataset [20], we compare against five recent SOTA low-light image enhancement methods (eight models in total) that are: EnlightenGAN [9], KinD++ [22], RUAS (RUAS-MIT5K and RUAS-LOL) [6], SCI (SCI-easy, SCI-medium and SCI-difficult) [7] and Zero-DCE++ [8].

Quantitative assessment is conducted using three full reference metrics (PSNR, SSIM, and LPIPS) and one no reference metric (NIQE [23]). The quantitative results reported in Table 1 show that LLDE achieves the top rank in both SSIM and LPIPS metrics, as well as 2nd rank in PSNR metric. LLDE’s ranks in these full reference metrics show its effectiveness in enhancing low-light images such that the enhanced images are almost identical to their respective ground truth images. Although LLDE’s performance in NIQE metric is somehow lower, note that NIQE [23] is designed to measure the deviations of the test images from statistical regularities observed in the natural images. As such, the LSRW test images that mainly consist of buildings or indoor scenes might not be suitable, we include the results of NIQE metric for reference and completeness.

For qualitative comparison, as illustrated in Figure 3, most SOTA models struggle to achieve a satisfactory level of expo-

sure, except for EnlightenGAN and our model. However, we can visualize that EnlightenGAN’s result is still slightly underexposed and suffers from noise.

An additional qualitative comparison is conducted on the NPE dataset [21], although the images sampled are not as severely underexposed as the LSRM dataset [20]. As depicted in Figure 4, EnlightenGAN produces artificial light glows. The image enhanced using KinD++ appears over-sharpened. The output from SCI’s easy and medium models exhibits either slight underexposure or overexposure. RUAS’s model, which was pre-trained with the LOL dataset over-enhances input, while the model pre-trained with the MIT-Adobe FiveK dataset suffers from color deviation. On the contrary, the rest of the models, including LLDE, produce a visually pleasing result. In summary, these examples demonstrate that LLDE can effectively enhance low-light images, which can pose challenges for other SOTAs.

However, LLDE is relatively slow, similar to most other diffusion-based generative models, due to their iterative nature. To illustrate, the runtime (GPU-seconds) of LLDE averaged on 20 images of size 960×640 is about 12 seconds, whereas other SOTAs can achieve subsecond runtime.

5. DISCUSSION AND CONCLUSION

To the best of our knowledge, LLDE is one of the earliest works to perform general low-light image enhancement using the diffusion model. It managed to produce competitive quantitative and qualitative results compared to recent SOTAs. Besides, LLDE has demonstrated the potential to be trained using unpaired low/normal-light images, as it delivers decent image enhancement when trained with misaligned image pairs in our experiment. Empirically, increasing diffusion time steps during sampling does not improve the enhancement results much, quantitatively and qualitatively. This observation aligns with the conclusion reached in [12].

6. REFERENCES

- [1] Chongyi Li, Chunle Guo, Linghao Han, Jun Jiang, Ming-Ming Cheng, Jinwei Gu, and Chen Change Loy, “Low-light image and video enhancement using deep learning: A survey,” *IEEE Transactions on Pattern Analysis and Machine Intelligence*, 2021.
- [2] Jascha Sohl-Dickstein, Eric A. Weiss, Niru Maheswaranathan, and Surya Ganguli, “Deep unsupervised learning using nonequilibrium thermodynamics,” *CoRR*, vol. abs/1503.03585, 2015.
- [3] Jonathan Ho, Ajay Jain, and Pieter Abbeel, “Denoising diffusion probabilistic models,” in *Advances in Neural Information Processing Systems*, H. Larochelle, M. Ranzato, R. Hadsell, M.F. Balcan, and H. Lin, Eds. 2020, vol. 33, pp. 6840–6851, Curran Associates, Inc.
- [4] Haidi Ibrahim and Nicholas Sia Pik Kong, “Brightness preserving dynamic histogram equalization for image contrast enhancement,” *IEEE Transactions on Consumer Electronics*, vol. 53, no. 4, pp. 1752–1758, 2007.
- [5] Edwin H Land, “The retinex theory of color vision,” *Scientific american*, vol. 237, no. 6, pp. 108–129, 1977.
- [6] Risheng Liu, Long Ma, Jiaao Zhang, Xin Fan, and Zhongxuan Luo, “Retinex-inspired unrolling with cooperative prior architecture search for low-light image enhancement,” in *Proceedings of the IEEE/CVF Conference on CVPR*, June 2021, pp. 10561–10570.
- [7] Long Ma, Tengyu Ma, Risheng Liu, Xin Fan, and Zhongxuan Luo, “Toward fast, flexible, and robust low-light image enhancement,” in *Proceedings of the IEEE/CVF Conference on Computer Vision and Pattern Recognition*, 2022, pp. 5637–5646.
- [8] Chongyi Li, Chunle Guo Guo, and Chen Change Loy, “Learning to enhance low-light image via zero-reference deep curve estimation,” in *IEEE Transactions on Pattern Analysis and Machine Intelligence*, 2021.
- [9] Yifan Jiang, Xinyu Gong, Ding Liu, Yu Cheng, Chen Fang, Xiaohui Shen, Jianchao Yang, Pan Zhou, and Zhangyang Wang, “Enlightengan: Deep light enhancement without paired supervision,” *IEEE Transactions on Image Processing*, vol. 30, pp. 2340–2349, 2021.
- [10] Yufei Wang, Renjie Wan, Wenhan Yang, Haoliang Li, Lap-Pui Chau, and Alex C Kot, “Low-light image enhancement with normalizing flow,” *arXiv preprint arXiv:2109.05923*, 2021.
- [11] Jiaming Song, Chenlin Meng, and Stefano Ermon, “Denoising diffusion implicit models,” *arXiv:2010.02502*, October 2020.
- [12] Alex Nichol and Prafulla Dhariwal, “Improved denoising diffusion probabilistic models,” *CoRR*, vol. abs/2102.09672, 2021.
- [13] Prafulla Dhariwal and Alexander Nichol, “Diffusion models beat gans on image synthesis,” in *Advances in Neural Information Processing Systems*, M. Ranzato, A. Beygelzimer, Y. Dauphin, P.S. Liang, and J. Wortman Vaughan, Eds. 2021, vol. 34, pp. 8780–8794, Curran Associates, Inc.
- [14] Chitwan Saharia, Jonathan Ho, William Chan, Tim Salimans, David J. Fleet, and Mohammad Norouzi, “Image super-resolution via iterative refinement,” *IEEE Transactions on Pattern Analysis and Machine Intelligence*, pp. 1–14, 2022.
- [15] Ozan Özdenizci and Robert Legenstein, “Restoring vision in adverse weather conditions with patch-based denoising diffusion models,” *IEEE Transactions on Pattern Analysis and Machine Intelligence*, pp. 1–12, 2023.
- [16] Yu Yuan, Jiaqi Wu, Lindong Wang, Zhongliang Jing, Henry Leung, Shuyuan Zhu, and Han Pan, “Learning to kindle the starlight,” 2022.
- [17] Diederik Kingma and Max Welling, “Auto-encoding variational bayes,” *ICLR*, 12 2013.
- [18] Olaf Ronneberger, Philipp Fischer, and Thomas Brox, “U-net: Convolutional networks for biomedical image segmentation,” *CoRR*, vol. abs/1505.04597, 2015.
- [19] Wenhan Yang Chen Wei, Wenjing Wang and Jiaying Liu, “Deep retinex decomposition for low-light enhancement,” in *British Machine Vision Conference*, 2018.
- [20] Jiang Hai, Zhu Xuan, Ren Yang, Yutong Hao, Fengzhu Zou, Fang Lin, and Songchen Han, “R2rnet: Low-light image enhancement via real-low to real-normal network,” *Journal of Visual Communication and Image Representation*, vol. 90, pp. 103712, 2023.
- [21] Shuhang Wang, Jin Zheng, Hai-Miao Hu, and Bo Li, “Naturalness preserved enhancement algorithm for non-uniform illumination images,” *IEEE Transactions on Image Processing*, vol. 22, no. 9, pp. 3538–3548, 2013.
- [22] Yonghua Zhang, Xiaojie Guo, Jiayi Ma, Wei Liu, and Jiawan Zhang, “Beyond brightening low-light images,” *International Journal of Computer Vision*, vol. 129, no. 4, pp. 1013–1037, Apr. 2021.
- [23] Anish Mittal, Rajiv Soundararajan, and Alan C. Bovik, “Making a “completely blind” image quality analyzer,” *IEEE Signal Processing Letters*, vol. 20, no. 3, pp. 209–212, 2013.